Appl. Phys. B 83, 285–288 (2006)
DOI: 10.1007/s00340-005-2106-9

Applied Physics B
Lasers and Optics

T. LAURILA[1,✉]
H. CATTANEO[1]
T. PÖYHÖNEN[1]
V. KOSKINEN[2]
J. KAUPPINEN[2]
R. HERNBERG[1]

Cantilever-based photoacoustic detection of carbon dioxide using a fiber-amplified diode laser

[1] Tampere University of Technology, Institute of Physics, Optics Laboratory, P.O. Box 692, 33101 Tampere, Finland
[2] University of Turku, Department of Physics, Laboratory of Optics and Spectroscopy, 20014 Turku, Finland

Received: 30 September 2005
Published online: 14 January 2006 •

ABSTRACT A compact and sensitive photoacoustic setup has been developed based on a recently demonstrated cantilever technique. A micromechanical cantilever transducer is attached to a cylindrical photoacoustic cell and the cantilever's deflection is monitored with a compact Michelson interferometer. A commercial 1-Watt optical fiber amplifier was used to enhance the performance of the system. A normalized sensitivity of 1.4×10^{-10} cm^{-1} W Hz$^{-1/2}$ was achieved in the detection of carbon dioxide at 1572 nm wavelength. Using 34 mW optical power from a DFB diode laser, the noise-equivalent detection limit for carbon dioxide at this wavelength is 4.0 ppm. Employing the fiber amplifier, we improved the sensitivity to yield measurement of sub-ppm concentrations.

PACS 42.62.Fi; 42.55.Px; 82.80.Ch

1 Introduction

Sensitive instruments are needed for gas detection in environmental, biological, medical, and industrial applications [1, 2]. Optical detection methods often provide high sensitivity [3] and narrow-band light sources enable molecule specific detection. Single-mode tunable diode lasers operating in the near infrared region are attractive light sources for sensitive and selective gas measurements. Such lasers, like distributed-feedback (DFB) diode lasers, are small, relatively robust and electronically fully controllable. Compactness of the sensor is a further desirable feature, in which sense photoacoustic spectroscopy (PAS) has good potential. PAS is a well-known technique for sensitive gas analysis [1, 4]. Lately, tunable diode laser based PAS (TDLPAS) has been proven a sensitive method [5, 6]. Several approaches have been used to improve the performance of TDLPAS setups, e.g., acoustic [7–9] and optical [10] resonances, fiber amplifier enhancement [5], and an intracavity configuration [11]. Minimum detectable absorption coefficients, $\alpha_{\min}$, obtained with TDLPAS are typically of the order of 10^{-8}–10^{-10} cm^{-1}.

The commercial availability of diode lasers with wavelengths matching the strongest molecular absorptions at fundamental vibrational bands in the mid-IR is still limited, although quantum cascade lasers operating at those wavelengths have fairly recently began to enter the market. Single-mode distributed-feedback diode lasers of high optical quality and reliability, developed mainly for telecom applications, are today readily available. These lasers match many of the overtone and combination molecular bands, but sensitivity is compromised by the weakness of these bands. Commercial fiber amplifiers (FAs) have developed rapidly during the last years driven by the telecommunication industry. These devices can be used to improve the sensitivity of the photoacoustic measurement in the near infrared [5]. Novel double-cladding fiber structures enable more powerful pumping of the amplifying fiber.

Recently, novel approaches for measuring the weak pressure waves inside a photoacoustic cell have been proposed [12–15]. A novel sensitive diode laser based photoacoustic setup utilizing an interferometrically-enhanced cantilever pressure transducer was recently demonstrated by Laurila et al. [16]. Using this technique a normalized sensitivity of 2.8×10^{-10} cm^{-1}W Hz$^{-1/2}$ for CO_2 detection at 1572 nm was achieved. In this work a completely new compact photoacoustic setup has been designed for a diode laser light source. The obtained noise-equivalent sensitivity for CO_2 diluted in argon is 1.4×10^{-10} cm^{-1}W Hz$^{-1/2}$. A commercial 1-Watt FA was also used to improve the system's performance.

2 Experimental

The experimental setup is shown in Fig. 1. Diode laser current and temperature drivers (ILX Lightwave LDX-3220 and LDT-5525) were used to tune the laser wave-

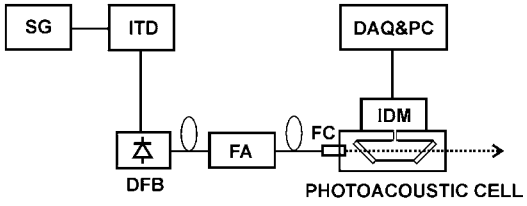

FIGURE 1 setup. SG–signal generator; ITD–current and temperature driver of the laser diode; DFB–distributed-feedback diode laser; FA–fiber amplifier; FC–fiber collimator; IDM–interferometric detection module; DAQ&PC–16-bit data acquisition board and personal computer

✉ Fax: +358 3 31152090, E-mail: toni.laurila@tut.fi

length to the desired absorption line. The fiber-pigtailed DFB diode laser (Furukawa Electric FOL 15DCWD-A81-19060) operating near 1572 nm had tuning parameters of 7.6×10^{-3} nm/mA and 9.8×10^{-2} nm/K. An ytterbium-erbium codoped fiber amplifier (IPG Photonics EAD-1K-L-SF) operating in the L band $\sim$ 1565–1610 nm was used to amplify the DFB laser output up to 1 W. The laser beam was collimated with a fiber collimator (Thorlabs F230FC-1550) to the diameter of 0.85-mm before entering the photoacoustic cell. The photoacoustic signals were detected using the interferometrically-enhanced micromechanical cantilever transducer [16].

CO_2 was chosen for the demonstration on the basis of laser and fiber amplifier availability. At 1572 nm CO_2 has a fairly weak vibrational combination band $[30^01]_{II}$. One of the strongest lines of this band at room temperature is the rotational line $R(18)$ at 1572.018 nm having a line intensity of 1.822×10^{-23} cm^{-1}/molec cm^{-2} [17]. The DFB laser was used for the excitation of CO_2 into the corresponding ro-vibrational state. Sinusoidal wavelength modulation was applied to sweep the laser line back and forth across the absorption line. This modulation technique generates a photoacoustic signal at twice the modulation frequency f_{mod}.

The magnitude of the photoacoustic signal [18] is given by

$$S_{\mathrm{PAS}} = C P_{\mathrm{opt}} \sigma n \tag{1}$$

where C is a constant depending on the pressure detection method, cell geometry, and modulation frequency, P_{opt} is the optical power of the excitation light source, σ is the absorption cross-section of the measured transition, and n is the number density of absorbing molecules. The constant C is usually defined by calibration, and it is proportional to the length of the cell l_{cell} and inversely proportional to the cell volume V_{cell} and the modulation frequency f_{mod}

$$C \propto \frac{l_{\mathrm{cell}}}{f_{\mathrm{mod}}\, V_{\mathrm{cell}}} \,. \tag{2}$$

The photoacoustic cell is shown in Fig. 2. The cell and the interferometric detection unit containing the cantilever were designed to be modular, i.e., the detection unit can be detached from the cell without any need to readjust the interferometer. The body of the cell and the interferometer module were made of aluminum. Fused silica windows are attached at Brewster's angle to minimize reflection losses in the case of linearly polarized input light. The cylindrical cell tube ($\varnothing = 3$ mm, $l = 40$ mm) was made of gold plated copper to minimize the effects of possible background absorption [19]. The sound generated by the photoacoustic effect is conducted to the cantilever through a 2.2 mm diameter hole in the side of the tube. The volume of the cell tube including small buffer volumes is 1.7 cm^3. The total absorption length in the cell is 6.1 cm, and the total volume of the cell including the gas inlet and outlet channels is about 3 cm^3. The response of the cantilever also depends on the volume behind it. However, if this volume is much larger than the cell volume then the effect on the cantilever's response is small. In this work the volume behind the cantilever was 17 cm^3. The photoacoustic setup was placed on a vibration isolated optical laboratory table to minimize the effects of building vibrations.

The dimensions of the cantilever used in this work were 6 mm × 2 mm × 10 μm (length, width and thickness). In our previous work [16] the dimensions were 4 mm × 2 mm × 5 μm, but cantilevers of this size were not available at the time of this study. The SOI (silicon-on-insulator) manufacturing process of the cantilever limited the thickness to 10 μm. The gap between the cantilever and its frame was 3 μm (earlier 30 μm) to enable the use of lower modulation frequencies. Changing of the gas sample may slightly change the temperature inside the cell. Therefore, to reduce the risk of breaking the cantilever's frame due to the different thermal expansion coefficients of aluminum and silicon the cantilever's frame was glued to a submount made of molybdenum, the thermal expansion coefficient of which is close to that of silicon.

The photoacoustic measurements were made in static gas conditions with a total pressure of 250 mbar. CO_2 was mixed with argon using calibrated mass flow controllers. The CO_2 concentration in argon was varied between 0 and 97.1 ppm. To change the gas sample the cell was first evacuated with a vacuum pump and then new sample gas was allowed to flow trough the cell for several minutes, after which the cell was closed. The photoacoustic cell was operated in non-

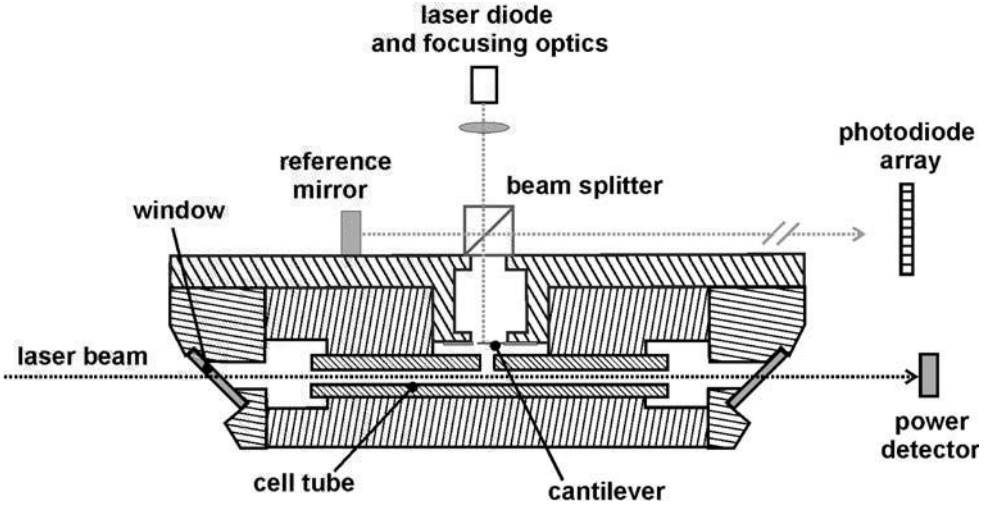

FIGURE 2 Photoacoustic cell and the detection setup. The cell tube (inner diameter 3 mm, 40 length) was made of copper and the inner surface was polished and gold plated

resonant mode using 20–100 Hz modulation frequencies. The resonance frequency of the cantilever was around 350 Hz at 250 mbar total pressure.

A compact optical Michelson interferometer was used to record the deflections of the cantilever. A 10 mm size 50 : 50 non-polarizing beam splitter cube was glued to the interferometer body (see Fig. 2). The beam of a 5 mW diode laser operating at 670 nm was focused through the beam splitter on the cantilever's free end. A reference mirror was adjusted to obtain a fringe pattern on three photodiodes of a photodiode array. The photodiode voltage signals were amplified and then subtracted from each other before the signals were acquired with a 16-bit data acquisition board. A Fourier transform of the cantilever signal was calculated using Labview software. The FT processing was not phase selective with respect to the wavelength modulation.

3 Results and discussion

The dependence of the photoacoustic signal at frequency $2f_{\mathrm{mod}}$ on CO_2 concentration is shown in Fig. 3. In this measurement a certified 97.1 ppm CO_2/Ar mixture ($\pm 1\%$ relative uncertainty) was diluted with argon of 99.9999% purity. In the measurements the DFB laser was operated at 34 mW. At each concentration the measured FFT spectrum is an average of 100 individual spectra corresponding to a measurement time of 75 s. A linear fit to the data gives a noise-equivalent (1σ) detection limit of 4.0 ppm.

The FA was used to increase the optical power of the DFB laser. The photoacoustic signals measured from CO_2 both in argon and nitrogen as a function of the FA's power are shown in Fig. 4. As evident from Fig. 4 the signal is linear with respect to the power, in accordance with (1). The measurements in argon were also made using two different modulation frequencies (39.65 and 87 Hz). As can be seen, the response is higher at lower modulation frequencies as expected according to (2). However, the noise from building vibrations increases with decreasing modulation frequency, which sets a lower limit to useful modulation frequencies.

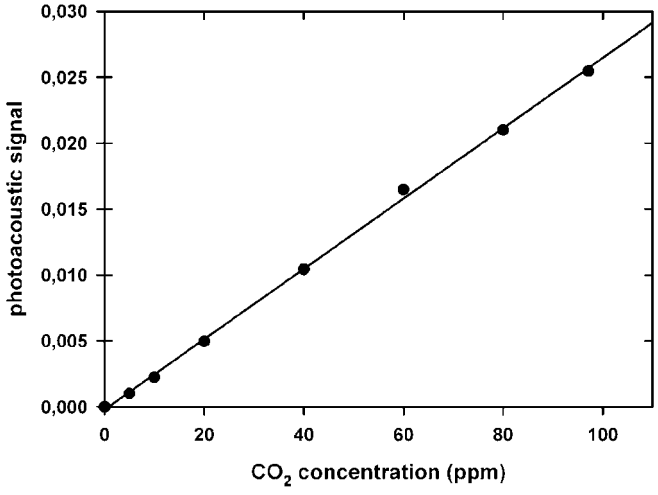

FIGURE 3 Photoacoustic signal as a function of the CO_2 concentration at 250 mbar total pressure. The DFB laser power in the measurements was 34 mW and the detection frequency was 79.3 Hz

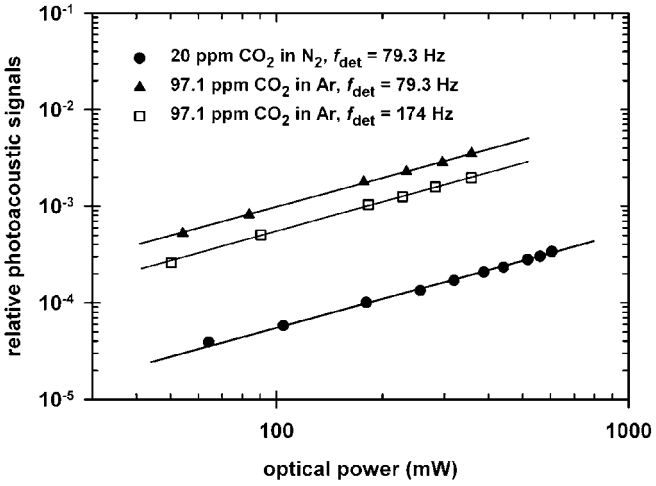

FIGURE 4 Photoacoustic signals from 97.1 ppm CO_2 diluted in argon and from 20 ppm CO_2 diluted in dry nitrogen as a function of the fiber amplifier's optical power. The photoacoustic signals from CO_2 mixed in argon were measured at two detection frequencies, 79.3 and 174 Hz ($f_{\mathrm{det}} = 2f_{\mathrm{mod}}$)

The best signal-to-noise ratios were obtained close to 40 Hz modulation frequency. We also observed that the photoacoustic response of CO_2 depends on the solvent gas. When using similar CO_2 concentrations the photoacoustic signals were approximately 60% lower in N_2 than in Ar. A similar observation at 1.43 μm wavelength has been made by Veres et al. [20] The suppression of the photoacoustic signal in N_2 is caused by molecular relaxation to a metastable state of N_2.

The nominal maximum output power of the FA was 1 W. A Glan–Taylor polarizer was placed between the FA's output and the cell window to eliminate background signals resulting from the reflection of polarization components not matching the Brewster angle of the cell windows. Otherwise, such background signals were observed in the Fourier spectrum both at frequencies f_{mod} and at $2f_{\mathrm{mod}}$ when the optical power was above 200 mW. These background signals were caused by the unwanted polarization components due to the input and output fibers of the FA, which were not polarization maintaining type. Using the fiber collimator and the polarizer, we found that the maximum power transmitted through the cell was 650–700 mW.

The transmitted polarization-controlled power changed considerably with the FA output power, because the polarization state of the amplifier output changed with the power in a more or less random way. Therefore, at each power level the FA's input and output fibers had to be twisted to equal the transmitted power to the set power value. The polarization related problems could be removed by using a FA having polarization maintaining fibers. However, even with the polarizer at optical power levels close to maximum some background signals were observed if the laser beam was not perfectly aligned through the 3 mm tube. A thin layer of nickel had been deposited under the gold plating to improve the long-term stability of the gold plating on copper. The quality of the gold plating inside the tube was good, but on the end surfaces of the tube the nickel layer was visible. Therefore, it is probable that when the laser beam was not properly aligned it was partially absorbed by the end sur-

Parameter	Prior work [16] CO_2 in N_2	This work CO_2 in Ar	
Excitation power (mW)	30	30	600
Detection frequency (Hz)	163	79.3	
Optical path length in the PA cell (cm)	20	6.1	
CO_2 detectivity (ppm)	7.9	4.6	0.23
Minimum detectable optical density, $\alpha_{\min} l$	1.8×10^{-8}	3.2×10^{-9}	1.6×10^{-10}
Minimum detectable absorption coefficient, $\alpha_{\min}$ (cm^{-1})	8.8×10^{-10}	5.2×10^{-10}	2.6×10^{-11}
Minimum normalized noise-equivalent sensitivity ($cm^{-1} W Hz^{-1/2}$)	2.8×10^{-10}	1.4×10^{-10}	

TABLE 1 Comparison of the results obtained in the prior work and in this work. All the figures of merit refer to noise-equivalent (1σ) values

Species	Wavelength (nm)	Line strength ($cm^{-1}/(molecule\,cm^{-2})$)	Detection limit
CO_2	1572.018	1.82×10^{-23}	4.6 ppm
CH_4	1654.561	1.21×10^{-21}	69 ppb
NH_3	1531.68	2.52×10^{-21}	33 ppb
CO	1568.036	2.31×10^{-23}	3.6 ppm

TABLE 2 Comparison between the attainable detection limits with the current setup for other gases absorbing in the near infrared. The first row shows the result obtained in this work. The inferred detection limits on the last three rows (noise equivalent values) have been calculated assuming 30 mW excitation power from a DFB laser. The spectral reference data for CO_2, CH_4, and CO are from [17] and for NH_3 from [21]

face of the tube and caused background signals. Thus, when low concentrations at high optical power levels are measured care must be taken to avoid any background signals due to absorption to the surfaces inside the cell or to the cell windows. Table 1 shows a summary of the results obtained in this work both using the DFB diode laser alone and with the FA. A comparison to the previous work is also made using different figures of merit. In Table 1 the DFB laser and the FA power are set to 30 mW and 600 mW, respectively.

The developed system can be rather easily applied to the measurement of other gases. Some gases absorbing in the near infrared region have stronger line intensities than CO_2. Table Table 2 shows predicted detection limits for some other gases absorbing in the near infrared where DFB diode lasers are commercially available. A 30 mW optical power has been assumed for the excitation light source. In the case of strongly absorbing gases the developed setup has potential to measure ppb level concentrations.

ACKNOWLEDGEMENTS The research was financially supported by the National Technology Agency of Finland (Tekes).

REFERENCES

1 M.W. Sigrist, *Air Monitoring by Spectroscopic Techniques* (John Wiley & Sons, New York 1994)
2 P. Hering, P. Lay, S.E. Stry, *Laser in Environmental and Life Sciences* (Springer, Berlin 2005)
3 J. Ye, L.S. Ma, J.L. Hall, J. Opt. Soc. Am. B **15**, 6 (1998)
4 A. Rosencwaig, *Photoacoustics and Photoacoustic Spectroscopy* (Robert E. Krieger Publishing, Florida 1990)
5 M.E. Webber, M. Pushkarsky, C.K.N. Patel, Appl. Opt. **42**, 2119 (2003)
6 A. Schmohl, A. Miklós, P.D. Hess, Appl. Opt. **41**, 1815 (2002)
7 A. Boschetti, D. Bassi, E. Iacob, S. Iannotta, L. Ricci, M. Scotoni, Appl. Phys. B **74**, 273 (2002)
8 Z. Bozóki, A. Mohácsi, G. Szabó, Z. Bor, M. Erdelyi, W.D. Chen, F.K. Tittel, Appl. Spectrosc. **56**, 715 (2002)
9 A. Miklós, M. Fehér, Infrared Phys. Technol. **37**, 21 (1996)
10 A. Rossi, R. Buffa, M. Scotoni, D. Bassi, S. Iannotta, A. Boschetti, Appl. Phys. Lett. **87**, 041110 (2005)
11 Z. Bozóki, J. Sneider, G. Szabó, A. Miklos, M. Serényi, G. Nagy, M. Fehér, Appl. Phys. B **63**, 399 (1996)
12 J. Kauppinen, K. Wilcken, I. Kauppinen, V. Koskinen, Microchem. J. **76**, 151 (2004)
13 K. Wilcken, J. Kauppinen, Appl. Spectrosc. **57**, 1087 (2003)
14 A.A. Kosterev, Y.A. Bakhirkin, R.F. Curl, F.K. Tittel, Opt. Lett. **27**, 1902 (2002)
15 A.A. Kosterev, F.K. Tittel, D.V. Serebryakov, A.L. Malinovsky, I.V. Morozov, Rev. Sci. Instrum. **76**, 043105 (2005)
16 T. Laurila, H. Cattaneo, V. Koskinen, J. Kauppinen, R. Hernberg, Opt. Exp. **13**, 2453 (2005)
17 L.S. Rothman, A. Barbe, D.C. Benner, L.R. Brown, C. Camy-Peyret, M.R. Carleer, K. Cjance, C. Clerbaux, V. Dana, V.M. Devi, A. Fayt, J.-M. Flaud, R.R. Gamache, A. Goldman, D. Jacquemart, K.W. Jucks, W.J. Lafferty, J.-Y. Mandin, S.T. Massie, V. Nemtchinov, D.A. Newnham, A. Perrin, C.P. Rinsland, J. Schroeder, K.M. Smith, M.A.H. Smith, K. Tang, R.A. Toth, J.V. Auwera, P. Varanasi, K. Yoshino, J. Quantum Spectrosc. Radiat. Transfer **82**, 5 (2003)
18 W. Demtröder, *Laser Spectroscopy* (Springer, Berlin 2003)
19 F.G.C. Bijnen, F.J.M. Harren, J.H.P. Hackstein, J. Reuss, Appl. Opt. **35**, 5357 (1996)
20 A. Veres, Z. Bozoki, A. Mohacsi, M. Szakall, G. Szabo, Appl. Spectrosc. **57**, 900 (2003)
21 M.E. Webber, D. Baer, R.K. Hanson, Appl. Opt. **40**, 2031 (2001)